MOLECULAR AND CELLULAR BIOLOGY, July 2010, p. 3165–3175 Vol. 30, No. 13
0270-7306/10/$12.00 doi:10.1128/MCB.00030-10

In Vivo Reconstitution of γ-Secretase in *Drosophila* Results in Substrate Specificity▽

Denise Stempfle,[1]† Ritu Kanwar,[2]† Alexander Loewer,[3]† Mark E. Fortini,[2] and Gunter Merdes[1]*

Department of Biosystems Science and Engineering, ETH Zürich, Mattenstr. 26, 4058 Basel, Switzerland[1]; Department of Biochemistry and Molecular Biology, Thomas Jefferson University, BLSB 830, 233 South 10th Street, Philadelphia, Pennsylvania 19107[2]; and Department of Systems Biology, Harvard Medical School, Boston, Massachusetts 02115[3]

Received 11 January 2010/Returned for modification 21 February 2010/Accepted 17 April 2010

The intramembrane aspartyl protease γ-secretase plays a fundamental role in several signaling pathways involved in cellular differentiation and has been linked with a variety of human diseases, including Alzheimer's disease. Here, we describe a transgenic *Drosophila* model for *in vivo*-reconstituted γ-secretase, based on expression of epitope-tagged versions of the four core γ-secretase components, Presenilin, Nicastrin, Aph-1, and Pen-2. In agreement with previous cell culture and yeast studies, coexpression of these four components promotes the efficient assembly of mature, proteolytically active γ-secretase. We demonstrate that *in vivo*-reconstituted γ-secretase has biochemical properties and a subcellular distribution resembling those of endogenous γ-secretase. However, analysis of the cleavage of alternative substrates in transgenic-fly assays revealed unexpected functional differences in the activity of reconstituted γ-secretase toward different substrates, including markedly reduced cleavage of some APP family members compared to cleavage of the Notch receptor. These findings indicate that *in vivo* under physiological conditions, additional factors differentially modulate the activity of γ-secretase toward its substrates. Thus, our approach for the first time demonstrates the overall functionality of reconstituted γ-secretase in a multicellular organism and the requirement for substrate-specific factors for efficient *in vivo* cleavage of certain substrates.

The Presenilin (PS) protein family was first identified on the basis of dominant familial mutations inducing early-onset Alzheimer's disease (26, 31, 37). An important pathological feature of Alzheimer's disease is the formation of plaques caused by the deposition of amyloid peptides derived from the proteolytic cleavage of the amyloid precursor protein (APP). The pathogenic Aβ peptide is produced by the sequential cleavage of APP through β- and γ-secretases (42). The first cleavage by β-secretase occurs at an extracellular site near the transmembrane region of APP, leading to secretion of the extracellular domain (ECD). The remaining C-terminal fragment (CTF) serves as a substrate for γ-secretase, which mediates proteolysis inside the membrane region, releasing the APP intracellular domain (AICD) and the Aβ peptide.

Soon after the identification of PS, its involvement in γ-secretase activity was revealed, and subsequently, a γ-secretase core complex was identified consisting of four proteins: PS, Nicastrin (Nct), anterior pharynx defective 1 (Aph-1) and PS enhancer 2 (Pen-2) (39). Strikingly, the γ-secretase complex responsible for cleaving APP comprises the same core components that are necessary for the cleavage of other transmembrane proteins, including Notch (21). Notch is the receptor in an evolutionarily conserved signaling pathway that plays a fundamental role in cellular differentiation and has been linked to a variety of diseases, including cancer (3, 17). Following ligand binding, the Notch receptor is cleaved at an extracellular site near its transmembrane domain, rendering the remaining CTF a substrate for the PS complex. Ultimately, the cleavage by the γ-secretase complex results in the release of the Notch intracellular domain (NICD), which engages in transcriptional regulation. This coordinated proteolysis of APP and Notch, as well as many other related type I integral membrane protein substrates, has been termed regulated intramembrane proteolysis (RIP) (4).

PS contains two aspartate residues that are essential for the catalytic activity of the complex and that are thought to form the active center of the protease (46). Nct, Aph-1, and Pen-2 contribute to the maturation and stabilization of the complex (24). Furthermore, evidence has been obtained for a function of Nct in substrate recognition (36), a view challenged by a recent study suggesting that Nct is instead needed only for maturation of the complex (7). Cell-based and cell-free assays have shown that only the coordinated overexpression of all four proteins leads to an increase in γ-secretase activity, arguing that they form the minimal active complex and that the assembly and maturation of the complex are highly regulated (39). In *Drosophila*, there is only one homolog of PS and Aph-1, whereas two homologs of each exist in mammalian cells (PS1/PS2 and Aph-1a/Aph-1b). Based on the fact that alternative *aph-1a* splice forms can be detected, it has been suggested, and subsequently demonstrated, that at least six distinct γ-secretase complexes exist in mammalian cells (38) that contribute to distinct γ-secretase activities (35). However, to date, the precise compositions and architectures of these complexes are not known, and depending on the experimental conditions used, complexes with a molecular mass of 250, 500, or >2,000 kDa have been isolated *in vitro*. Recently, it was

* Corresponding author. Mailing address: Department of Biosystems Science and Engineering, ETH Zürich, Mattenstr. 26, 4058 Basel, Switzerland. Phone: 41(0)613873142. Fax: 41(0)613873994. E-mail: gunter.merdes@bsse.ethz.ch.

† D.S., R.K., and A.L. contributed equally to this work.

▽ Published ahead of print on 16 April 2010.

TABLE 1. Functional verification of the epitope-tagged γ-secretase components PS, Nct, and Aph-1 used for transgenic expression studies[a]

Transgene	Epitope tag	Expression method	Mutant allele tested	Degree of rescue
Psn-loopmyc	Myc	*presenilin* promoter fusion	*psnB3*	Complete
Psn-Nmyc	Myc	*presenilin* promoter fusion	*psnB3*	Complete
Nct-2myc	Myc	*daughterless-GAL4*::*UAS*	*nctJ1*	Complete
		hsp70-GAL4::*UAS*	*nctJ1*	Partial
Aph1-V5	V5	*tubulin-GAL4*::*UAS*	*aph1D35*	Complete
		armadillo-GAL4::*UAS*	*aph1D35*	Partial

[a] The mutant alleles used are lethal amorphs having no detectible genetic activity, with lethality occurring at stage P4(i) during the initial larval-pupal transition. Complete rescue is defined as the production of viable, morphologically normal adults; partial rescue is defined as survival beyond stage P4(i) with morphogical evidence of further pupal development, but lethal prior to the adult stage.

shown that a complex containing only one of each component displays *in vitro* activity, but it is unknown whether this activity is found *in vivo* as well (33). Furthermore, recently published interactome analyses of γ-secretase suggest that it interacts with a variety of other proteins, which could be important for maturation, localization, and/or enzymatic activity (43, 44). Taken together, these findings illustrate a potential limitation with the analysis of purified γ-secretase complexes, namely, that their observed *in vitro* minimal activities might not fully reflect their full range of activities and cleavage efficiencies *in vivo*.

In one of the earliest models addressing PS activity and specificity, it was suggested that substrate recognition by the γ-secretase complex depends only on the size of the ECD and is sequence independent (40). To address this phenomenon in more detail, we developed a reporter system in *Drosophila* which monitors the cleavage of transmembrane proteins *in vivo* during *Drosophila* development, and we showed that PS-mediated cleavage of APP is regulated in a cell-type-specific manner, independent of the size of the ECD (27). In the meantime, several studies have confirmed the existence of complex regulatory mechanisms that influence the cleavage efficiencies of different substrate CTFs (8, 9, 18).

To address the question of the activity of the core PS complex and the contribution of substrate-specific factors, we reconstituted the *Drosophila* PS complex *in vivo* by simultaneous overexpression of tagged versions of the four core components with the GAL4/upstream activation sequence (UAS) system (15) and analyzed its ability to cleave alternative model substrates, including ones based on Notch and different APP/APLP family members. In contrast to mammalian γ-secretase, *Drosophila* γ-secretase is homogenous in composition due to the fact that single-copy genes encode each of its four core subunits. Our *Drosophila*-based approach thus permits the analysis of substrate-specific cleavage efficiencies without the additional complication of multiple potential γ-secretase complexes having distinct enzymatic properties. We found that *in vivo*-reconstituted *Drosophila* γ-secretase displayed biochemical and cell biological features similar to those of endogenous γ-secretase but exhibited substrate-specific effects with respect to its proteolytic activities toward Notch and APP/APLP proteins. These findings have potential implications for understanding the diverse functions of γ-secretase involving different cleaved substrates in different tissues, as well as the development of pharmacological inhibitors that could potentially target specific substrates.

MATERIALS AND METHODS

***Drosophila* transgene construction and creation of transgenic fly lines.** Unless otherwise stated, standard *Drosophila* genetic and molecular biology techniques were used. Substrates for the fluorescent RIP-detecting *in vivo* reporter system were cloned by recombination and analyzed using Leica SP5 or SP2 confocal systems as described previously (27). Transgenic fly lines for γ-secretase-R (see below) were established according to standard procedures by subcloning epitope-tagged γ-secretase component cDNA inserts (described in reference 23) into the *Drosophila* transformation vector pUAST for UAS/GAL4 expression to create UAS-Psn-loopmyc, UAS-Psn-Nmyc, UAS-Nct-2myc, UAS-Aph1-V5, and UAS-Pen2-2flag flies or into the pPEPC vector (34) for direct transcriptional fusion to the endogenous PS promoter to create PEPC-Psn-loopmyc and PEPC-Psn-Nmyc flies (Table 1). Several individual lines were tested for each construct.

Biochemical analyses. For protein immunoblots from fly heads, flies were frozen in liquid nitrogen and heads were separated from thoraxes by vigorous shaking and knocking the tubes onto a hard surface. The fly heads were collected and directly transferred into 3 μl 2× SDS sample buffer (containing 3.5 M urea) per fly head. After the addition of 3 μl Benzonase (Merck or Roche) per 10 fly heads, the tissue was homogenized in 1.5-ml reaction tubes using a micropestle (Eppendorf), incubated at 37°C for 15 min, and centrifuged at 16,000 × *g* for 10 min, and up to 30 μl was loaded onto NuPAGE Novex Bis-Tris Mini Gels (Invitrogen). After PAGE, the proteins were transferred onto Hybond membranes (Amersham) by tank blotting in 25 mM Tris, 192 mM glycine, 20% methanol at 200 mA for 2.5 h at 4°C. The membranes were washed with phosphate-buffered saline (PBS) plus 0.05% Tween 20 (PBST), blocked with PBST plus 5% milk powder (PBST-MP) (Applichem), and incubated with the respective antibodies in PBST-MP overnight at 4°C. The membranes were then washed with PBST, incubated with secondary antibodies (ECL Western Blotting Detection System; Amersham) in PBST-MP for 2 h at room temperature (RT), and washed with PBST. Bound antibodies were detected with the ECL Western Blotting Detection System (Amersham), and signals were visualized with hyperfilm (Amersham). Alternatively, bound antibodies were visualized with Super-Signal West Femto (Thermo). Published protocols for mammalian γ-secretase were applied to fly head homogenates: coimmunoprecipitation (co-IP) and tandem affinity (19), size exclusion chromatography (22), continuous density gradient centrifugation (49) (glycerol was replaced by sucrose), and blue native (BN)-PAGE (33). The isolation of subcellular compartments utilized a protocol established for mammalian cells (2). The sucrose step gradients were assembled by successively layering differently concentrated sucrose solutions (in HEPES-EDTA [5 mM HEPES, pH 7.0, 1 mM EDTA]) on top of each other in 14- by 89-mm tubes at 4°C. The following standardized protocol was utilized to perform the actual experiments: >0.2 g of fly heads was incubated with 2 ml buffer HO (5 mM HEPES, pH 7.0, 250 mM sucrose, 1 mM EDTA, 1× Roche Complete-EDTA-Free) per 0.1 g heads on ice for 5 min in a Wheaton homogenizer and then homogenized on ice (10 times with a loose pestle/2 times with a tight pestle). The homogenate was transferred into 15-ml Falcon tubes and centrifuged 3 times for 10 min each time at 500 × *g*, and 1 to 1.3 ml of the postnuclear supernatant was layered on top of the prepared sucrose gradients. The gradients were centrifuged at 274,000 × *g* (40,000 rpm; TH-641 rotor [Thermo]) for 2 h at 4°C, and 500-μl fractions were collected from the bottom. The distribution of cellular compartments was determined based on the distribution profiles of different marker proteins: Rab5, Rab7, Rab11, LAMP1, KDEL-receptor, GM130, β′-COP, and Calnexin. Except for the anti-β′-COP antibody, all antibodies are published or commercially available material. The anti-β′-COP antibody was raised in rabbits using a β′-COP–glutathione *S*-transferase (GST) fusion protein

(G. Merdes, unpublished data). The distribution of these marker proteins was used to refine the original gradient into a gradient that consisted of 10 steps with different sucrose concentrations, which gave better resolution of endosomal compartments (see Fig. 2).

Antibody production. Selection of immunogenic peptides and immunization of rabbits to generate antibodies for *Drosophila* Aph-1, Pen-2, and Nct was done by Peptide Specialty Laboratories GmbH, Heidelberg, Germany. The following peptides were used: Pen-2, MDISKAPNPRKLELC/CAFHKPPFSEQSQIKR/CTNRTAWGATADYMSFIIPLGSA; Aph-1, RSTEQGLHAVAEDTRVTDNKHC/MSGPGTMGLKGGTEC/AFDTNNYIHC/CAGGTSRSFRKFITCQ; Nct, RTNQMKQFSHELNC/LERLNNYAKSPRYGFC/ARPTNKYYHSIYDDADNVC/CSRSEVLFEDLPASNAALFG.

The anti-PS-loop and anti-PS-NTF antibodies were raised in rabbits using a PS-loop- and a PS-NTF-GST fusion protein.

RESULTS AND DISCUSSION

***In vivo* reconstitution of *Drosophila* γ-secretase.** Previous studies demonstrated that expression of the four *Drosophila* γ-secretase components, PS, Nct, Aph-1, and Pen-2, in *Drosophila* S2 is sufficient for efficient assembly of mature, functional γ-secretase (23, 41). To investigate the activities of reconstituted γ-secretase *in vivo*, we expressed these four components in transgenic flies using the binary GAL4/UAS expression system (see Materials and Methods). In *Drosophila*, the well-established GAL4/UAS system allows the expression of transgenes in precise spatiotemporal patterns during development and in the adult fly (15). This method not only facilitates studying the function and subcellular localization of a gene product in a cell-type-specific manner, but also can be used for the isolation and characterization of protein complexes (30). Therefore, we generated UAS-transgenic constructs for PS, Nct, Aph-1, and Pen-2 fused to different epitope tags. To verify that each cDNA used for these constructs was functional and that insertion of epitope tags did not compromise the activity of the encoded proteins, we tested the ability of each transgene to rescue the lethal phenotype of the respective *Drosophila* mutants. Using GAL4 driver lines to drive the UAS transgenes in widespread or ubiquitous expression patterns or the endogenous fly PS gene promoter to express the Myc-tagged PS constructs, we found that transgenically expressed PS, Nct, and Aph-1 are each capable of fully rescuing the lethality and associated mutant phenotypes of the corresponding *Drosophila* loss-of-function genetic mutants (Table 1). For the Pen-2-expressing transgene, we were unable to test for functional genetic rescue due to the lack of available mutations in the endogenous *Drosophila pen-2* gene.

Having established that the transgenically expressed, tagged γ-secretase components possessed *in vivo* activity, we tested for γ-secretase reconstitution and subcomplex formation by expressing different transgene combinations in the *Drosophila* eye. This tissue is especially suitable for the characterization of membrane proteins due to its high membrane content and suitability for biochemical studies (16, 20, 29). Furthermore, the *Drosophila* eye is a well-established system to model neurodegenerative diseases, including Alzheimer's disease (28), and requires Notch signaling and, thus, γ-secretase activity for its development (5). Fly stocks were created in which different combinations of UAS-PS (with a Myc tag), UAS-Nct (with a Myc tag), UAS-Aph-1 (with a V5 tag), and UAS-Pen-2 (with a FLAG tag) were expressed under the control of the widely used eye-specific GMR-GAL4 driver line. Unless otherwise indicated, these UAS/GAL4 transgene combinations were used for all the studies described below.

Fly heads of the different genotypes were isolated and subjected to SDS-PAGE and protein immunoblot analysis. As displayed and quantified in Fig. 1A and B, expression of certain combinations of transgenes led to the formation of subcomplexes, as reflected by specific changes in protein stability; for instance, Aph-1 increased the stability of coexpressed full-length PS or coexpressed Nct. Simultaneous expression of all three proteins (PS, Nct, and Aph-1) resulted in a further increase in stability (Fig. 1A). In contrast, Pen-2 became detectable only upon coexpression with PS. The expression of all four components resulted in a massive increase in the amount, and thus stability, of Pen-2, and high-level activity of the complex became apparent through the striking enrichment of N- and C-terminal PS fragments (PS-CTF and PS-NTF), generated through endoproteolysis, and a concomitant decrease in levels of the full-length protein (Fig. 1A).

Molecular characteristics of *in vivo*-reconstituted γ-secretase. To verify the presence of a reconstituted γ-secretase complex (termed γ-secretase-R) in these fly head homogenates, we performed IPs and tandem-affinity purification with antibodies recognizing the Myc tag, FLAG tag, or Aph-1 (Fig. 1C to E). Both strategies resulted in the reproducible co-IP of other complex partners, indicating that a fully assembled and potentially functional γ-secretase-R was present.

A variety of molecular techniques have been used to characterize γ-secretase, including size exclusion chromatography and density gradient centrifugation. To gain further insight into the characteristics of our reconstituted complex, we applied these techniques to extracts prepared from wild-type flies expressing endogenous γ-secretase (termed γ-secretase-E), as well as the transgenically reconstituted γ-secretase-R flies. Size exclusion chromatography revealed a size for human γ-secretase of >500 kDa, with a large proportion of the γ-secretase complexes having a size of >670 kDa (47). Under comparable experimental conditions, the elution profiles for *Drosophila* γ-secretase-E and -R were almost identical (Fig. 1F). Similarly, density gradient centrifugation indicated a size of approximately 800 to 900 kDa for γ-secretase-R (Fig. 1G). In comparison, a theoretical monomeric γ-secretase complex in *Drosophila* would be expected to have a molecular mass of 175 kDa. Pretreatment of the complex with Triton X-100 resulted in partial disassembly of this complex and especially promoted the dissociation of Pen-2 (Fig. 1H). Density gradient centrifugation in the presence of the detergent CHAPSO resulted in a distribution profile that indicated a γ-secretase complex of approximately 280 kDa (Fig. 1I), in line with results for human γ-secretase (49). Thus, using different techniques, we showed that the size of the recombinant complex corresponded to published values.

To assess the similarities and differences in the subcellular distributions of γ-secretase-E and -R, we performed immunohistochemical analyses at different time points in the development of the *Drosophila* eye. However, the small size of the visualized cells and the inability of the anti-Pen-2 antibodies to specifically recognize the protein in this assay led to inconclusive results (data not shown). Previously, sucrose density gradient centrifugation procedures have been applied, not only to vertebrate cells and tissues, but also to *Drosophila* cells and fly

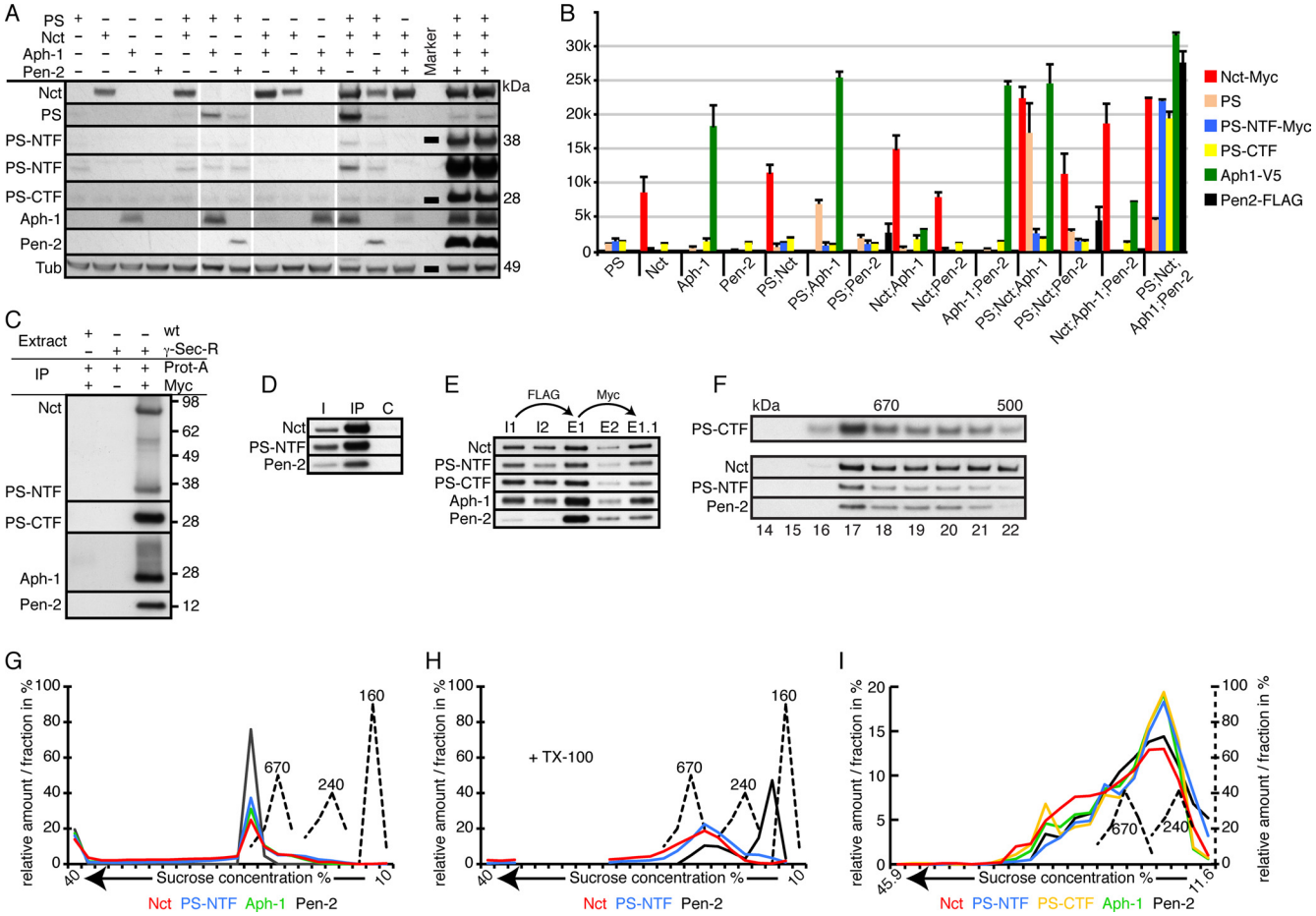

FIG. 1. Molecular characteristics of *in vivo*-reconstituted γ-secretase. If not otherwise indicated, homogenates from adult fly heads expressing GAL4 under the control of *GMR* were used in this and all following figures. (A) Protein immunoblot analyses of fly heads expressing the indicated γ-secretase components. For PS-NTF, two different exposure times are shown, with the longer exposure beneath the shorter exposure. Tubulin (Tub) served as the loading control for these samples. (B) Histogram showing the quantification (plus standard deviations [SD]) of the normalized amounts of the different γ-secretase-R components detected in panel A. PS-CTF was present in all genotypes, as the antibody used recognized endogenous, as well as transgenically expressed, PS-CTF. (C) Co-IP of γ-secretase-R (γ-sec-R) components with protein A-Sepharose (Prot-A) and anti-Myc antibodies, which recognize the Myc epitope tags on transgenically expressed PS and Nct. wt, wild type. (D) Co-IP of γ-secretase-R components with an antibody raised against a peptide epitope of Aph-1. I, input; C, control (nonfunctional anti-Aph-1 antibody). (E) Co-IP and tandem purification of γ-secretase-R components. In the first step, the complex was enriched using anti-FLAG antibodies that recognize transgenically expressed Pen-2 and eluted with FLAG-peptide (E1 and E2). The eluted complex was then further purified with anti-Myc antibodies that recognize transgenically expressed PS and Nct and eluted using Myc peptide (E1.1). I1 and E1, input and eluate from detergent-extracted total fly heads; I2 and E2, input and eluate from detergent-extracted membrane preparations. (F) Protein immunoblot analyses of fractions from size exclusion chromatography. On top, the elution profile for γ-secretase-E is shown (PS-CTF). Below is the profile for γ-secretase-R, probed with antibodies to the three individual components shown on the left. (G and H) Diagrams of the distribution profiles of γ-secretase-R in continuous sucrose gradients with or without Triton X-100 (TX-100). The molecular masses of marker proteins are displayed in kDa. The distribution profile of each component is color coded to match the corresponding component shown at the bottom. (I) Diagram of the distribution profile of γ-secretase-R in a continuous sucrose gradient containing the detergent CHAPSO, with unit scales and color coding as in panel F. Antibodies used: anti-Myc recognizing transgenic Nct and PS-NTF, anti-V5 recognizing transgenic Aph-1, anti-FLAG recognizing transgenic Pen-2, and anti-PS-loop recognizing endogenous and transgenic PS and PS-CTF.

head homogenates to isolate and separate different cellular compartments (1, 2, 6, 25). We therefore applied these experimental procedures (2) to fly head homogenates containing γ-secretase-E and -R and obtained almost identical subcellular distribution profiles for both (Fig. 2B). However, detailed analyses of the distributions of marker proteins for the different endosomal compartments revealed very limited resolution of these intracellular structures under the standard gradient conditions (Fig. 2A). Accordingly, we adjusted the protocol and developed a sucrose density gradient procedure that resulted in an optimized distribution and separation of the endoplasmic reticulum (ER), Golgi apparatus, and endosomal membranes (Fig. 2C). Within these gradients, the distribution profiles for the components of γ-secretase-E and -R were almost identical, albeit the detection of endogenous Pen-2 was at the sensitivity limit (Fig. 2D). Both types of γ-secretase displayed a predominant localization to fractions positive for the late endosomal marker Rab7 and the recycling endosomal marker Rab11 (Fig. 2D).

In summary, the applied experimental procedures and tech-

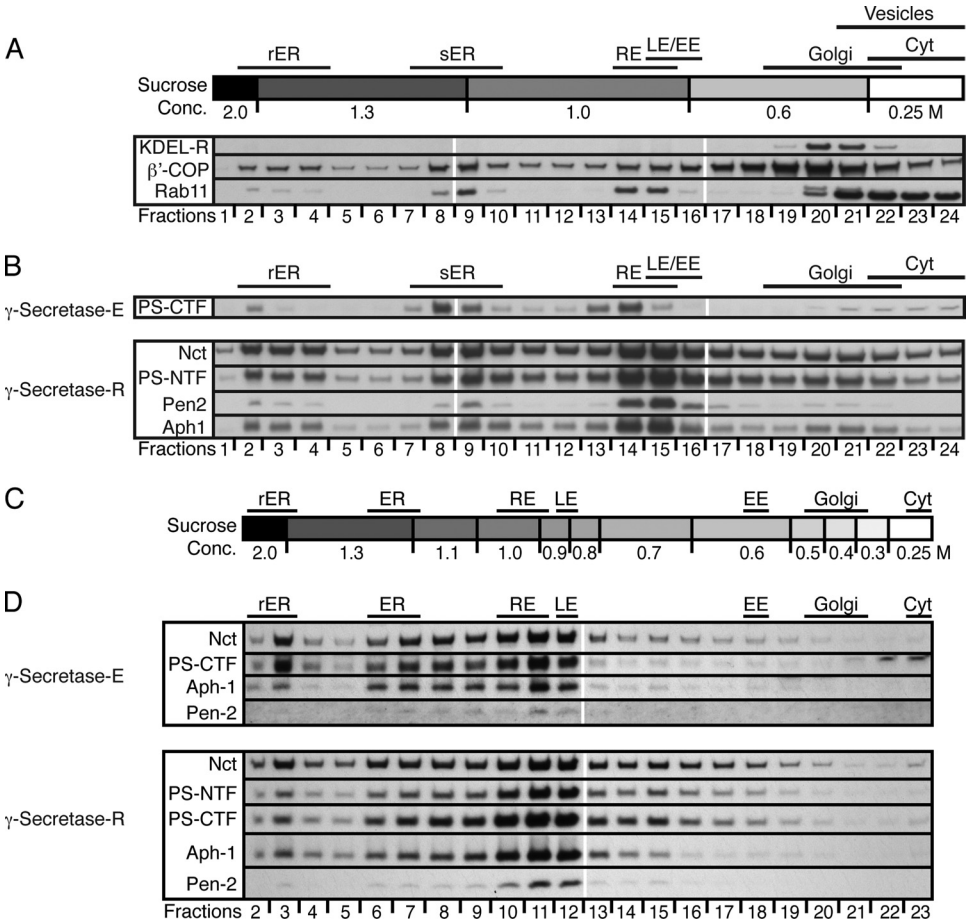

FIG. 2. Subcellular localization of *Drosophila* γ-secretase-R in the adult eye. (A) Representative examples of protein immunoblots of postnuclear adult head extracts from control flies fractionated on a sucrose step gradient, revealing the distribution of intracellular compartment marker proteins KDEL-R, β′-COP, and Rab11. The respective fraction numbers and the corresponding sucrose concentrations (Conc.) are given at the top and bottom. The distribution profile for Rab11 overlaps with a previously published distribution profile and fits the known associations of Rab11 with synaptic vesicles, recycling endosomes, and the ER. (B) Protein immunoblots of postnuclear adult head extracts from control (γ-secretase-E-expressing) and γ-secretase-R-expressing flies fractionated on sucrose step gradient I. On top, the localizations of different intracellular compartments, characterized by the presence of certain marker proteins and enzymes within the fraction(s), are indicated. At the bottom, the respective fraction numbers and the corresponding sucrose concentrations are given. The individual γ-secretase components being monitored in each immunoblot are given on the left. (C) The distribution of intracellular compartment marker proteins was used to refine the sucrose gradient to achieve a better resolution of the endosomal compartments. (D) Protein immunoblots of postnuclear adult head extracts from control (γ-secretase-E-expressing) and γ-secretase-R-expressing flies fractionated on the refined sucrose step gradient, showing the distribution of each γ-secretase component indicated on the left. The corresponding fraction numbers (bottom) and intracellular compartment markers (top) are denoted. The antibodies used were the same as for Fig. 1. rER, rough endoplasmic reticulum; ER, smooth endoplasmic reticulum; RE, recycling endosomes; LE, late endosomes; EE, early endosomes; Golgi, Golgi apparatus; Cyt, cytosol.

niques showed that the endogenous and the reconstituted *Drosophila* γ-secretases are almost indistinguishable and revealed that *Drosophila* γ-secretase exhibits a subcellular distribution similar to that of its human counterpart.

Functional properties of reconstituted γ-secretase. Different assays have been described in the literature to test for γ-secretase activity, and in many cases, *in vitro* assays have been used that rely on the cleavage of bacterially expressed substrates. Several previous analyses of reconstituted γ-secretase have been performed *in vitro* using mammalian, *Drosophila*, and yeast cell-based assays (12). Our creation of transgenic animals expressing all four γ-secretase core components needed for enzymatic activity allowed us to investigate the physiological properties of the reconstituted complex *in vivo* with respect to the cleavage of endogenous γ-secretase substrates and the signaling pathways whose outputs depend on γ-secretase activity. To this end, we visualized the cleavage of the *Drosophila* APP homolog APPL by protein immunoblot analyses of head extracts from wild-type flies and flies expressing γ-secretase-R. As depicted in Fig. 3, expression of γ-secretase-R consistently resulted in increased APPL-ICD production. However, the amount of ICD was very small due to rapid degradation, and thus, the strong reduction in the amounts of APPL-CTFs through the activity of γ-secretase-R served as a more reliable indicator for enhanced γ-secretase activity (Fig. 3A and B), analogous to the reduction in human APP C99 fragment levels caused by γ-secretase (48).

As previously mentioned, PS activity is a classical feature of

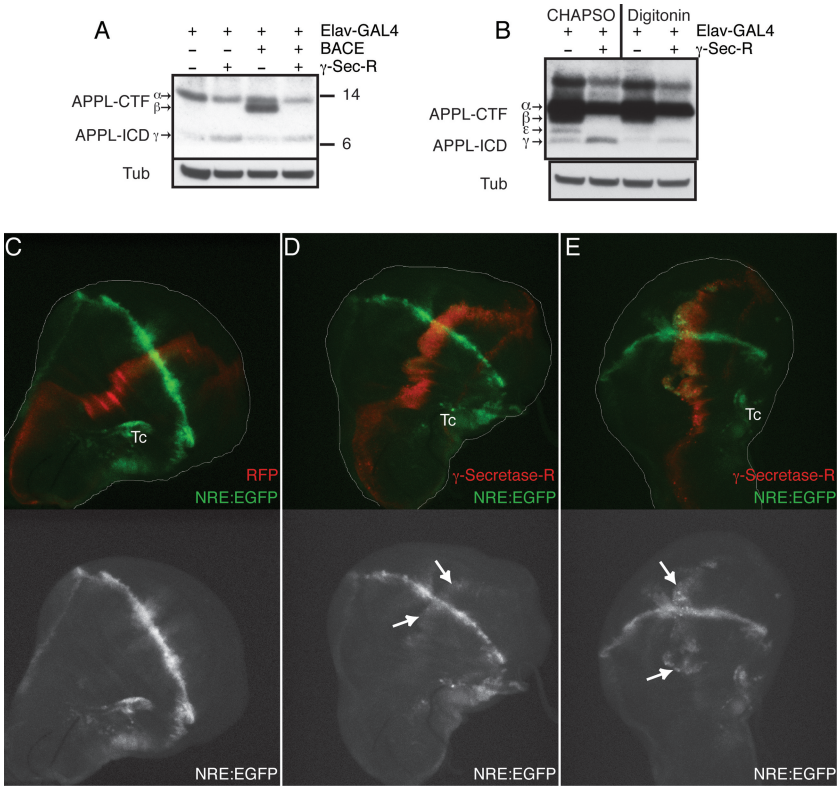

FIG. 3. Enhanced proteolysis of APPL and stimulated Notch signaling by γ-secretase-R. (A) Protein immunoblots of supernatants obtained from fly heads of the indicated genotype following hypotonic lysis and SDS-PAGE. Transgenic expression of human BACE results in an APPL-CTF (β; arrow at left), which is shorter than the CTF generated by endogenous α-secretase activity (α; arrow at left). Nevertheless, both CTFs are recognized as substrates by γ-secretase-R, which cleaves them into a smaller ICD fragment (γ; arrow at left). Tub, tubulin loading control. (B) Protein immunoblots of extracts obtained from fly heads of the indicated genotypes using different detergents, as indicated at the top. Only in the presence of CHAPSO was a clear increase in the amount of ICD observed, whereas the amount of CTF was similarly decreased by γ-secretase-R with either detergent. No effect was observed on the amount of full-length APPL (data not shown). (C to E) Maximum projections of confocal sections (z stacks) of wing imaginal discs from wild-type control animals (C) or transgenic animals expressing γ-secretase-R (D and E) examined for Notch pathway activity. EGFP expression (green) reflects the output of the Notch signaling pathway along the dorsal-ventral boundary, visualized using the Notch reporter NRE-EGFP. RFP expression (red) indicates the expression domain of ptc-GAL4 and thus monitors the coexpressed γ-secretase-R. Images are shown as pairs with the overlay in color and the EGFP channel separately in black and white. The arrows mark areas with enhanced Notch signaling output, although slight changes (as in the middle row) are more apparent with *in vivo* imaging, which avoids the photobleaching caused by confocal scan recording. Autofluorescent tracheae are indicated (Tc).

the canonical Notch signaling pathway, essential for Notch receptor cleavage and signal transduction across the animal kingdom. In the developing *Drosophila* wing, Notch activation leads to the localized Suppressor of Hairless [Su(H)]-dependent expression of target genes, such as *cut* and *Enhancer of Split* [*E*(*spl*)] (10). This observation has been used to generate a reporter for Notch activity based on the *Notch response element* (*NRE*)-driven expression of CD2 (11). We cloned the *NRE* from the aforementioned Notch reporter, inserted it upstream of *EGFP*, and generated transgenic fly lines bearing this *NRE-EGFP* fluorescent reporter (32a). In these flies, enhanced green fluorescent protein (EGFP) expression marked the cells with active Su(H)-dependent Notch signaling along the dorsal-ventral boundary during wing development *in vivo* (Fig. 3C and D). We then combined this transgene with *patched*-GAL4 (*ptc*-GAL4) and UAS-red fluorescent protein (RFP). Crossing the resulting line into the γ-secretase-R transgenic background restricted γ-secretase-R expression to the RFP-marked stripe of *patched*-expressing cells along the anterior-posterior compartment of the wing disc (Fig. 3C). Comparison of control wing discs to wing discs expressing γ-secretase-R revealed a substantial increase in Notch reporter expression in the *patched* expression domain in 15% of the flies (Fig. 3E) and a weak increase in an additional 30% ($n = 30$) (Fig. 3D). Such changes were never observed in control discs ($n = 40$) (Fig. 3C). Accordingly, we conclude that our γ-secretase-R is active *in vivo* and that increases in the amount of γ-secretase result in enhanced APPL cleavage and elevated Notch signaling.

To address whether overexpression of γ-secretase results in observable morphological phenotypes, we selected a variety of GAL4 lines and used them to express γ-secretase-R in different tissues during *Drosophila* development. Table 2 gives an overview of the targeted tissues and the phenotypic consequences. Taken together, even high-level overexpression of γ-secretase in tissues such as the eye and the wing did not induce any obvious phenotypic consequences. In contrast, the global overexpression of γ-secretase-R during embryogenesis,

TABLE 2. Phenotypes induced by γ-secretase-R overexpression during *Drosophila* development

GAL4 driver	GAL4 expression pattern	Phenotype
tubulin	High expression in all cells, starting from early embryogenesis	Larval lethality
rhomboid	Expression in mesectoderm during embryogenesis, in the central nervous system (CNS), and in the photoreceptor cells	Lethal
armadillo	Moderate expression in all cells, starting from early embryogenesis	Partial lethality (reduced hatching rate)
179y	Expression in a segmentally repeated pattern of stripes during late embryogenesis and in the larva in the CNS and the lamina anlagen (near the central brain boundary)	Partial lethality (reduced hatching rate)
vestigal	Expression along the dorsal-ventral boundary of the wing disc	None
distalless	Expression in distal portions of leg and antenna discs and along the dorsal-ventral boundary of the wing disc	None
nanos	Maternally deposited in the embryo	None
scabrous	Expression in sensory organ precursors	None
GMR	Very high expression anterior to the morphogenetic furrow in all cells of the developing and adult eye	None
apterous	Expression in the dorsal compartment of the wing disc and in the nervous system	Curved wing, vein defects

for instance, with *tubulin*-GAL4, resulted in lethality, suggesting interference with key developmental processes that are very sensitive to the amount of γ-secretase.

Substrate specificity of reconstituted γ-secretase. Studying the functionality of γ-secretase-R *in vivo* using endogenous substrates is hampered by the fact that RIP is a tightly regulated process heavily depending on the activities of other proteases that first cleave and remove the extracellular domains of potential substrates. We therefore developed a reporter system to detect RIP directly with engineered γ-secretase substrates that lack their normal inhibitory extracellular domains. This reporter system (27) takes advantage of the inability of a transcription factor to enter the nucleus if it is fused to the intracellular domain (ICD) of a transmembrane protein (Fig. 4A and B). For γ-secretase substrates, it is the cleavage by this enzyme that liberates the ICD, resulting in the translocation of the chosen transcription factor to the nucleus and expression of target genes. In our case, we used a synthetic transcription factor consisting of the LexA DNA binding domain and the VP16 transcriptional activation domain (LexA-VP16) and a LexA-Operator sequence governing the expression of GFP as a reporter. To monitor γ-secretase activity independently of any proceeding extracellular proteolytic events, we generated flies transgenic for a potential direct γ-secretase substrate termed αNotch (αN) (Fig. 4B), which corresponds to the Notch transmembrane domain lacking the large Notch extracellular and intracellular domains. As shown in Fig. 4D and E, the expression of γ-secretase-R resulted in a striking elevation in reporter activity with this substrate. This enhanced activity persisted into adulthood and could be visualized by protein immunoblot analysis, as well (Fig. 4F). Furthermore, we established the specificity of the reporter system with respect to γ-secretase activity by culturing eye discs *in vitro* in the presence or absence of the γ-secretase-specific inhibitor *N*-[*N*-(3,5-difluorophenacetyl)-L-alanyl]-*S*-phenylglycine *t*-butyl ester (DAPT) or compound E (Fig. 4G and data not shown). To confirm that the observed enhanced γ-secretase activity did indeed depend on the full γ-secretase-R, we assessed the activities of the single components, as well as different combinations, using the reporter system. Interestingly, overexpression of PS alone resulted in visibly enhanced γ-secretase activity, which nevertheless was considerably lower than the activity obtained with the reconstituted complex (Fig. 4H). Expression of Nct and Aph-1 alone or in combination had almost no effect. These results suggest that the amount of PS is rate limiting for the activity of endogenous *Drosophila* γ-secretase in the eye imaginal disc and that reconstituted γ-secretase-R is fully functional.

To extend these findings to other substrates, we monitored the effect of γ-secretase-R on human APP and APLP2 with the reporter system *in vivo* (Fig. 5). APLP2 is a human APP paralog that also undergoes RIP (14). Surprisingly, APP cleavage was consistently downregulated in γ-secretase-R flies (Fig. 5). However, as we used full-length proteins, no judgment can be made about the effect being direct (involving substrates not recognized by γ-secretase-R) or indirect (involving interference with the preceding extracellular cleavage[s]). We addressed this point by devising two additional α constructs, termed α*APP* and α*APLP2* (Fig. 5), which are membrane-anchored ICD variants lacking the extracellular domains, analogous to αN described above. Expression of α*APP* in the absence or presence of reconstituted γ-secretase resulted in the same activity pattern obtained with the full-length protein, namely, a strong decrease in αAPP cleavage in the presence of γ-secretase-R, whereas we observed a slight increase in αAPLP2 cleavage (Fig. 5). We find it physiologically unlikely that APP-ICD acts as a transcriptional activator when released by γ-secretase-E yet as a repressor when released by γ-secretase-R, and we effectively ruled this possibility out by generating and testing αAPP-APLP2 chimeric proteins (Fig. 5). Neither the replacement of the APP-ICD with the APLP2-ICD nor the replacement of the transmembrane or extracellular domain changed the outcome of the experiment. Thus, two conclusions can be drawn: first, APLP2 can be cleaved by γ-secretase-R; however, as we did not observe an increase in reporter expression, as in the case of αN, cleavage by γ-secretase is unlikely to be the rate-limiting step for downstream transcriptional events. Second, APP is evidently not an optimal *in vivo* physiological substrate for γ-secretase-R. Given the high overexpression of γ-secretase-R in our assays, one can assume that endogenous complexes are fully replaced by reconstituted complexes, and thus effective cleavage of APP is disabled.

These findings raise the question of whether αAPP is not a substrate for γ-secretase-R due to impairment of substrate

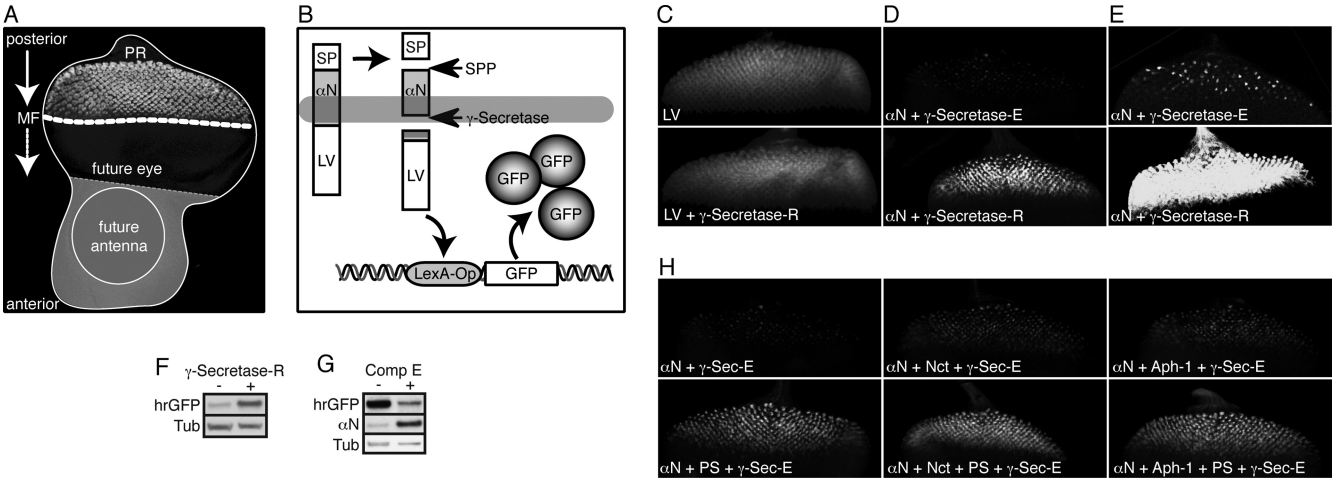

FIG. 4. Visualization of enhanced γ-secretase activity *in vivo*. (A) Assembled confocal image of a *Drosophila* eye-antenna imaginal disc isolated from a late-third-instar larva. The disc was labeled with an antibody against the neuronal marker Elav, mainly localizing to the nucleus of photoreceptor neurons (PR) within the developing retina. In this larval stage, a morphogenetic furrow (MF) moves from posterior to anterior within the presumptive eye epithelium. Behind this furrow, and thus in reciprocal direction to the movement of the MF, the differentiation of photoreceptor clusters occurs, resulting in columns containing progressively more mature groups of differentiating cells. The GMR enhancer drives expression of GAL4 in all cells posterior to the morphogenetic furrow. (B) Schematic representation of the reporter system that permits the *in vivo* detection of intramembrane proteolysis at the cellular level. Expression of an engineered optimal Notch-based γ-secretase substrate (αN) is induced with GMR-GAL4. This type I transmembrane protein contains a truncated extracellular domain and is fused at its intracellular C terminus to the synthetic transcription factor LexA-VP16 (LV). Thus, cleavage by the signal peptide peptidase (SPP) mimics extracellular shedding and induces the concomitant release of a membrane-anchored CTF. This CTF is recognized by γ-secretase as a substrate, which results in its intramembrane proteolysis and the release of the intracellular fragment ICD. The synthetic transcription factor LV domain fused to the ICD then translocates to the nucleus, resulting in its binding to the LexA-Operator sequence present in the transgenic reporter construct. As a consequence, GFP expression is induced specifically in only those cells with recent and/or ongoing γ-secretase activity. (C) Maximum projections of confocal sections of eye imaginal discs expressing γ-secretase-R together with the reporter system to detect the activity of soluble LV. Depicted is the output of the reporter system (GFP fluorescence) in the absence (top) and presence (bottom) of γ-secretase-R, and no effect of γ-secretase-R on LV activity could be observed. The images were recorded simultaneously under identical conditions. (D) Maximum projections of confocal sections of eye imaginal discs expressing γ-secretase-R together with the reporter system to detect the intramembrane cleavage of αN. Depicted is the output of this cleavage-dependent reporter system (GFP fluorescence) in the absence (top) and presence (bottom) of γ-secretase-R. The images were recorded simultaneously under identical conditions. (E) Experiment similar to that in panel D, but the imaging conditions were adjusted to allow enhanced visualization of the signal generated by γ-secretase-E. (F) αN reporter larvae possessing γ-secretase-E but lacking γ-secretase-R (−) and αN reporter larvae expressing γ-secretase-R (+) were allowed to develop to adults, and their adult heads were subjected to protein immunoblot analyses to visualize changes in GFP expression (hrGFP) indicative of overall γ-secretase proteolytic activity. Tub, tubulin loading control. (G) Protein immunoblots from eye imaginal discs expressing the αN reporter system alone, which were cultured *in vitro* in the absence or presence of the γ-secretase inhibitor compound E (Comp E). Inhibition of γ-secretase-E resulted in an increase in the amount of uncleaved substrate and a concomitant decrease in GFP expression. (H) Maximum projections of confocal sections of eye imaginal discs from transgenic larvae in which different combinations of individual γ-secretase-R components were coexpressed in conjunction with the αN cleavage reporter system, as indicated at the bottom left of each image. Depicted is the output of the reporter system (GFP fluorescence) in each genotype. The images were recorded under identical conditions.

localization, impaired substrate recognition and/or docking to the complex, or impaired substrate cleavage. Using the aforementioned techniques of size exclusion chromatography and sucrose density centrifugation, we did not observe any differences in the distribution profiles of αAPP in the presence or absence of γ-secretase-R (Fig. 6A and B). Therefore, we performed co-IPs from fly head homogenates expressing αAPP and γ-secretase-R, as well as extracts from flies expressing LexA-VP16 and αAPLP2 that served as controls (Fig. 6C). Pulldown of γ-secretase-R with anti-FLAG resulted in the copurification of αAPP. In comparison, no LexA-VP16 and only minor amounts of αAPLP2 were copurified. Furthermore, for αAPLP2, two protein bands could be detected, suggesting cleavage and concomitant release of this substrate during the procedure. In the reverse experiment, the IP of αAPP using an anti-VP16 antibody resulted in the copurification of Nct and PS-NTF in larger amounts (Fig. 6D). Previously, it has been reported that co-IP of APP CTFs with human γ-secretase occurs only when the enzyme is inactivated (48), which, together with our results, implies that γ-secretase-R recognizes αAPP as a substrate but is unable to catalyze its proteolysis.

To gain further insight into the molecular characteristics of the γ-secretase-R complex(es) that binds to αAPP, we performed BN-PAGE, following a previously published protocol (33). Fly head homogenates of various genotypes were subjected to BN-PAGE, and the distributions of αAPP and γ-secretase-E and -R were visualized by using the respective antibodies in protein immunoblot analyses (Fig. 6E). Interestingly, whereas for γ-secretase-E we detected only one complex with an approximate size of 190 kDa, two complexes were detected for γ-secretase-R, with approximate sizes of 190 and 117 kDa, with the larger complex predominating. Furthermore, if one compares the ratios in the distributions of the

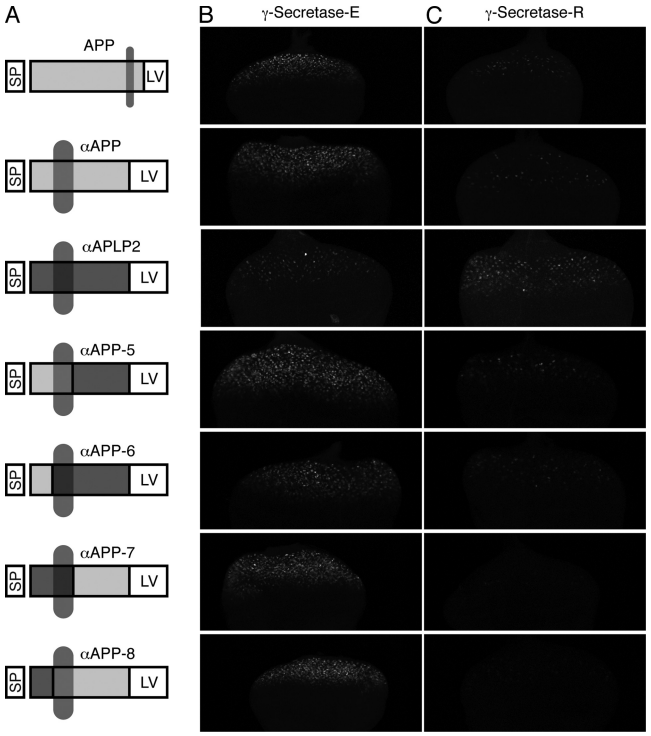

FIG. 5. Substrate specificity of γ-secretase-R. (A) Schematic representation of the γ-secretase substrates APP, αAPP, and αAPLP2 and of the various chimeras generated by domain swapping between αAPP and αAPLP2. Important protein domains are highlighted. (B and C) Maximum projections of confocal sections of eye imaginal discs of larvae with cleavage reporters based on engineered APP and APLP2 γ-secretase-optimized substrates. Depicted is the output of the reporter system (GFP fluorescence) in the absence (B) and presence (C) of γ-secretase-R and with full-length APP, αAPP, or αAPLP2 as a substrate. The images were recorded simultaneously under identical conditions.

different components in each complex, an underrepresentation of PS-NTF and Pen-2 in the smaller complex becomes evident, suggesting that this complex mainly contains Nct, PS-CTF, and Aph-1. It is intriguing, however, that αAPP seems to be enriched in this smaller, 117-kDa complex whereas in the control sample we observed αAPP enrichment in the larger, 190-kDa complex (Fig. 6E). Hence, it is tempting to speculate that αAPP associates predominantly with an inactive form of γ-secretase, which would explain why its cleavage is impaired in our transgenic-fly reporter assays. However, the co-IP experiments clearly revealed that αAPP also associated with the fully assembled γ-secretase-R without being cleaved. This finding raises the possibility that the smaller complex represents an immature form of the γ-secretase and that premature recruitment of αAPP during complex assembly results in cleavage inhibition even if the complex is fully assembled eventually or that the smaller complex is a nonfunctional degradation product of γ-secretase. The latter possibility would indicate that expression of the γ-secretase core components is sufficient to assemble a functional enzyme but that the efficient cleavage of some substrates depends on additional factors, which are not expressed at adequate levels in our transgenic animals. We favor this model, not only because the expression of the components in different double and triple combinations did not affect αAPP cleavage in the same manner as simultaneous expression of all four components (data not shown), but also because there is no obvious reason why αN and αAPLP2 should not assemble with immature forms of γ-secretase as well. Furthermore, this interpretation is consistent with the fact that immature forms of the complex, including those we observed, contain Nct, which has been proposed to play a key role in substrate recruitment/docking.

Currently, the requirement for substrate-specific factors for the cleavage of proteins by γ-secretase is an intriguing topic in the field of Alzheimer's disease-related research. Due to the contributions of PS to Notch and other physiologically important signaling pathways, global inhibition of γ-secretase is considered unfavorable as a therapy, as it would cause unacceptable side effects (45). In contrast, substrate-specific factors would be ideal targets for therapeutic intervention. One prominent substrate-specific factor identified previously is TMP21, a member of the p24 protein family involved in vesicle transport. TMP21 was identified as a γ-secretase component and was demonstrated to inhibit cleavage of APP at the γ site (8).

Further studies will be required to identify the factor(s) that must be coexpressed with γ-secretase to ensure efficient cleavage of APP by the core complex in *Drosophila*. These factors might include proteins, as well as lipids or other molecules, generated or modified by the fly genome. To isolate such factors, forward genetic approaches, as well as biochemical approaches, can be employed. For example, comparing the spectrum of proteins copurifying with active γ-secretase-E to those associating with γ-secretase-R could lead to the identification of key cofactors. Subsequently, these proteins could be overexpressed with γ-secretase-R and their effects on cleavage efficiency could be monitored with the *in vivo* reporter system. The reporter system could also be used to perform a comprehensive genetic screen to identify second-site mutations that influence γ-secretase-R cleavage efficiency in *Drosophila*. In this approach, flies expressing γ-secretase-R, the reporter system, and αAPP as a substrate would be crossed to a collection of fly lines carrying random transposon insertions, termed EP elements. EP elements contain upstream activation sequences, as well as a core promoter capable of driving GAL4-dependent transcription of genomic DNA sequences adjacent to the site of insertion (32). Consequently, randomly targeted genes can be overexpressed, enabling new genes and gene functions to be identified based on their overexpression phenotypes, a strategy that has been successfully exploited to dissect developmental processes and signaling pathways (13). In the envisioned genetic screen, an increase in αAPP cleavage-dependent GFP expression would serve as a sensitive readout for novel genes that influence γ-secretase activity. Factors identified by these methods could subsequently be studied in more detail in *Drosophila* and in mammalian model systems.

In summary, our approach for the first time demonstrates the overall functionality of reconstituted γ-secretase in a multicellular organism and the requirement for substrate-specific factors for efficient *in vivo* cleavage of certain substrates. Our findings can now serve as a starting point to apply the powerful

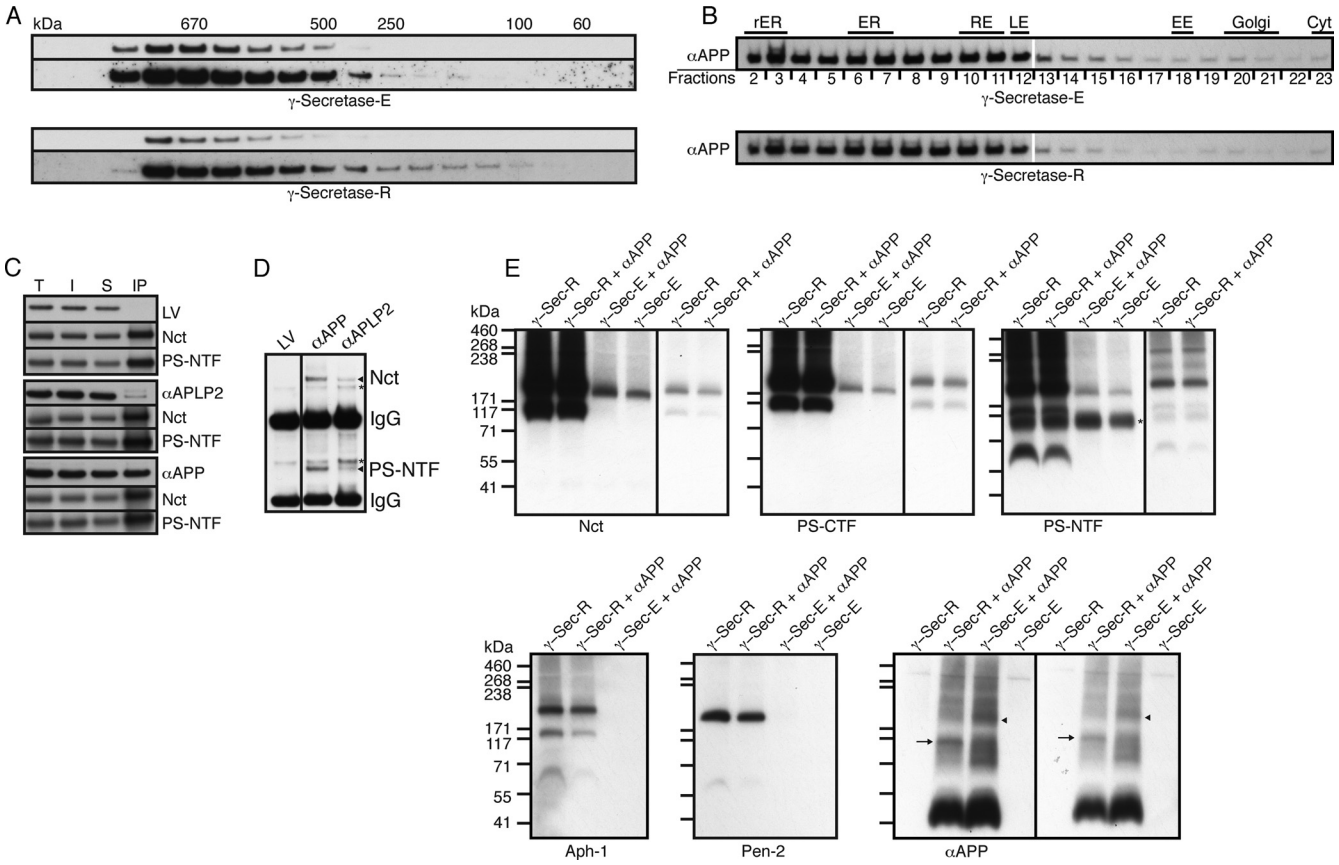

FIG. 6. Molecular characteristics and subcellular localization of αAPP. (A) Protein immunoblot analyses of fractions from size exclusion chromatography in the absence (γ-secretase-E; top) and presence (bottom) of γ-secretase-R. Two different exposure times are displayed for each case, with the longer exposure below the shorter one. No differences in the elution profiles were observed. (B) Protein immunoblots of postnuclear adult head extracts from control (γ-secretase-E-expressing) and γ-secretase-R-expressing flies fractionated on a sucrose step gradient. No obvious differences in the distribution profiles of αAPP in the presence or absence of γ-secretase-R were observed with either gradient protocol, indicating that the expression of γ-secretase-R changes neither the molecular characteristics nor the subcellular localization of αAPP. Abbreviations of subcellular compartments are as in Fig. 2. (C) Protein immunoblots of IPs with anti-FLAG antibodies recognizing transgenically expressed Pen-2–FLAG from extracts containing γ-secretase-R and either LexA-VP16 (LV), αAPP, or αAPLP2. T, total; I, input; S, supernatant after IP. Nct and PS-NTF were detected with an anti-Myc antibody and LV, αAPP, and αAPLP2 with an anti-VP16 antibody. (D) Protein immunoblot of IPs from the extracts in panel C performed with an anti-VP16 antibody. Nct and PS-NTF (arrowheads) were visualized using an anti-Myc antibody. Nonspecific bands detected by the anti-Myc antibody are marked with asterisks. (E) Protein immunoblots of extracts separated by BN-PAGE, with the corresponding extract genotypes indicated above and the proteins being monitored shown below each immunoblot. In some cases, two different exposure times are presented for certain lanes, with the shorter exposure in a separate box at the right. The arrow in the αAPP immunoblot marks an enrichment of αAPP at the position of a smaller γ-secretase-R complex, whereas the arrowhead denotes the position corresponding to γ-secretase-E. A nonspecific band detected by the anti-Myc antibody is marked with an asterisk in the PS-NTF immunoblot. Antibodies used for the detection of the indicated proteins in panel D: Nct, anti-Nct; PS-CTF, anti-PS-Loop; PS-NTF, anti-PS-NTF; Aph-1, anti-V5; Pen-2, anti-FLAG; αAPP, anti-VP16.

forward genetics and molecular tools of *Drosophila* to gain further insights into γ-secretase function and regulation.

ACKNOWLEDGMENTS

We gratefully acknowledge Renato Paro for his support.

G.M. is supported by the DFG and the Alzheimer Forschung Initiative e.V. (AFI). M.E.F. is supported by NIH grant GM087650 and the Department of Biochemistry and Molecular Biology, Thomas Jefferson University.

REFERENCES

1. **Adolfsen, B., S. Saraswati, M. Yoshihara, and J. T. Littleton.** 2004. Synaptotagmins are trafficked to distinct subcellular domains including the postsynaptic compartment. J. Cell Biol. **166:**249–260.
2. **Bole, D. G., L. M. Hendershot, and J. F. Kearney.** 1986. Posttranslational association of immunoglobulin heavy chain binding protein with nascent heavy chains in nonsecreting and secreting hybridomas. J. Cell Biol. **102:** 1558–1566.
3. **Bolós, V., J. Grego-Bessa, and J. L. de la Pompa.** 2007. Notch signaling in development and cancer. Endocr. Rev. **28:**339–363.
4. **Brown, M. S., J. Ye, R. B. Rawson, and J. L. Goldstein.** 2000. Regulated intramembrane proteolysis: a control mechanism conserved from bacteria to humans. Cell **100:**391–398.
5. **Cagan, R. L., and D. F. Ready.** 1989. Notch is required for successive cell decisions in the developing Drosophila retina. Genes Dev. **3:**1099–1112.
6. **Cermelli, S., Y. Guo, S. P. Gross, and M. A. Welte.** 2006. The lipid-droplet proteome reveals that droplets are a protein-storage depot. Curr. Biol. **16:** 1783–1795.
7. **Chávez-Gutiérrez, L., A. Tolia, E. Maes, T. Li, P. C. Wong, and B. de Strooper.** 2008. Glu(332) in the Nicastrin ectodomain is essential for gamma-secretase complex maturation but not for its activity. J. Biol. Chem. **283:** 20096–20105.
8. **Chen, F., H. Hasegawa, G. Schmitt-Ulms, T. Kawarai, C. Bohm, T. Katayama, Y. Gu, N. Sanjo, M. Glista, E. Rogaeva, Y. Wakutani, R. Pardossi-Piquard, X. Ruan, A. Tandon, F. Checler, P. Marambaud, K. Hansen, D.**

Westaway, P. St George-Hyslop, and P. Fraser. 2006. TMP21 is a presenilin complex component that modulates gamma-secretase but not epsilon-secretase activity. Nature **440:**1208–1212.
9. **Coolen, M. W., K. M. van Loo, N. N. van Bakel, B. A. Ellenbroek, A. R. Cools, and G. J. Martens.** 2006. Reduced Aph-1b expression causes tissue- and substrate-specific changes in gamma-secretase activity in rats with a complex phenotype. FASEB J. **20:**175–177.
10. **de Celis, J. F., A. Garcia-Bellido, and S. J. Bray.** 1996. Activation and function of Notch at the dorsal-ventral boundary of the wing imaginal disc. Development **122:**359–369.
11. **de Celis, J. F., D. M. Tyler, J. de Celis, and S. J. Bray.** 1998. Notch signalling mediates segmentation of the Drosophila leg. Development **125:**4617–4626.
12. **De Strooper, B.** 2003. Aph-1, Pen-2, and Nicastrin with Presenilin generate an active gamma-Secretase complex. Neuron **38:**9–12.
13. **Duchek, P., K. Somogyi, G. Jekely, S. Beccari, and P. Rorth.** 2001. Guidance of cell migration by the Drosophila PDGF/VEGF receptor. Cell **107:**17–26.
14. **Eggert, S., K. Paliga, P. Soba, G. Evin, C. L. Masters, A. Weidemann, and K. Beyreuther.** 2004. The proteolytic processing of the amyloid precursor protein gene family members APLP-1 and APLP-2 involves alpha-, beta-, gamma-, and epsilon-like cleavages: modulation of APLP-1 processing by N-glycosylation. J. Biol. Chem. **279:**18146–18156.
15. **Elliott, D. A., and A. H. Brand.** 2008. The GAL4 system: a versatile system for the expression of genes. Methods Mol. Biol. **420:**79–95.
16. **Eroglu, C., P. Cronet, V. Panneels, P. Beaufils, and I. Sinning.** 2002. Functional reconstitution of purified metabotropic glutamate receptor expressed in the fly eye. EMBO Rep. **3:**491–496.
17. **Fortini, M. E.** 2009. Notch signaling: the core pathway and its posttranslational regulation. Dev. Cell **16:**633–647.
18. **Fraering, P. C., W. Ye, M. J. LaVoie, B. L. Ostaszewski, D. J. Selkoe, and M. S. Wolfe.** 2005. Gamma-secretase substrate selectivity can be modulated directly via interaction with a nucleotide-binding site. J. Biol. Chem. **280:** 41987–41996.
19. **Fraering, P. C., W. Ye, J. M. Strub, G. Dolios, M. J. LaVoie, B. L. Ostaszewski, A. van Dorsselaer, R. Wang, D. J. Selkoe, and M. S. Wolfe.** 2004. Purification and characterization of the human gamma-secretase complex. Biochemistry **43:**9774–9789.
20. **Gnagey, A. L., M. Forte, and T. L. Rosenberry.** 1987. Isolation and characterization of acetylcholinesterase from Drosophila. J. Biol. Chem. **262:**13290–13298.
21. **Hass, M. R., C. Sato, R. Kopan, and G. Zhao.** 2009. Presenilin: RIP and beyond. Semin. Cell Dev. Biol. **20:**201–210.
22. **Hoke, D. E., J. L. Tan, N. T. Ilaya, J. G. Culvenor, S. J. Smith, A. R. White, C. L. Masters, and G. M. Evin.** 2005. In vitro gamma-secretase cleavage of the Alzheimer's amyloid precursor protein correlates to a subset of presenilin complexes and is inhibited by zinc. FEBS J. **272:**5544–5557.
23. **Hu, Y., and M. E. Fortini.** 2003. Different cofactor activities in gamma-secretase assembly: evidence for a nicastrin-Aph-1 subcomplex. J. Cell Biol. **161:**685–690.
24. **Kaether, C., C. Haass, and H. Steiner.** 2006. Assembly, trafficking and function of gamma-secretase. Neurodegener. Dis. **3:**275–283.
25. **Khodosh, R., A. Augsburger, T. L. Schwarz, and P. A. Garrity.** 2006. Bchs, a BEACH domain protein, antagonizes Rab11 in synapse morphogenesis and other developmental events. Development **133:**4655–4665.
26. **Levy-Lahad, E., W. Wasco, P. Poorkaj, D. M. Romano, J. Oshima, W. H. Pettingell, C. E. Yu, P. D. Jondro, S. D. Schmidt, K. Wang, et al.** 1995. Candidate gene for the chromosome 1 familial Alzheimer's disease locus. Science **269:**973–977.
27. **Loewer, A., P. Soba, K. Beyreuther, R. Paro, and G. Merdes.** 2004. Cell-type-specific processing of the amyloid precursor protein by Presenilin during Drosophila development. EMBO Rep. **5:**405–411.
28. **Lu, B., and H. Vogel.** 2009. Drosophila models of neurodegenerative diseases. Annu. Rev. Pathol. **4:**315–342.
29. **Oliver, D. V., and J. P. Phillips.** 1970. Fruit fly fractionation. Drosophila Inf. Serv. **45:**58.
30. **Parker, L., S. Gross, and L. Alphey.** 2001. Vectors for the expression of tagged proteins in Drosophila. Biotechniques **31:**1280–1282, 1284, 1286.
31. **Rogaev, E. I., R. Sherrington, E. A. Rogaeva, G. Levesque, M. Ikeda, Y. Liang, H. Chi, C. Lin, K. Holman, T. Tsuda, et al.** 1995. Familial Alzheimer's disease in kindreds with missense mutations in a gene on chromosome 1 related to the Alzheimer's disease type 3 gene. Nature **376:**775–778.
32. **Rørth, P., K. Szabo, A. Bailey, T. Laverty, J. Rehm, G. M. Rubin, K. Weigmann, M. Milan, V. Benes, W. Ansorge, and S. M. Cohen.** 1998. Systematic gain-of-function genetics in Drosophila. Development **125:**1049–1057.
32a. **Saj, A., Z. Arziman, D. Stempfle, W. van Belle, U. Sauder, T. Horn, M. Dürrenberger, R. Paro, M. Boutros, and G. Merdes.** 2010. A combined ex vivo and in vivo RNAi screen for Notch regulators in Drosophila reveals an extensive Notch interaction network. Dev. Cell doi:10.1016/j.devcell.2010.03.013.
33. **Sato, T., T. S. Diehl, S. Narayanan, S. Funamoto, Y. Ihara, B. De Strooper, H. Steiner, C. Haass, and M. S. Wolfe.** 2007. Active gamma-secretase complexes contain only one of each component. J. Biol. Chem. **282:**33985–33993.
34. **Seidner, G. A., Y. Ye, M. M. Faraday, W. G. Alvord, and M. E. Fortini.** 2006. Modeling clinically heterogeneous presenilin mutations with transgenic Drosophila. Curr. Biol. **16:**1026–1033.
35. **Serneels, L., J. Van Biervliet, K. Craessaerts, T. Dejaegere, K. Horre, T. Van Houtvin, H. Esselmann, S. Paul, M. K. Schafer, O. Berezovska, B. T. Hyman, B. Sprangers, R. Sciot, L. Moons, M. Jucker, Z. Yang, P. C. May, E. Karran, J. Wiltfang, R. D'Hooge, and B. De Strooper.** 2009. Gamma-secretase heterogeneity in the Aph1 subunit: relevance for Alzheimer's disease. Science **324:**639–642.
36. **Shah, S., S. F. Lee, K. Tabuchi, Y. H. Hao, C. Yu, Q. LaPlant, H. Ball, C. E. Dann III, T. Sudhof, and G. Yu.** 2005. Nicastrin functions as a gamma-secretase-substrate receptor. Cell **122:**435–447.
37. **Sherrington, R., E. I. Rogaev, Y. Liang, E. A. Rogaeva, G. Levesque, M. Ikeda, H. Chi, C. Lin, G. Li, K. Holman, et al.** 1995. Cloning of a gene bearing missense mutations in early-onset familial Alzheimer's disease. Nature **375:**754–760.
38. **Shirotani, K., D. Edbauer, S. Prokop, C. Haass, and H. Steiner.** 2004. Identification of distinct gamma-secretase complexes with different APH-1 variants. J. Biol. Chem. **279:**41340–41345.
39. **Steiner, H., R. Fluhrer, and C. Haass.** 2008. Intramembrane proteolysis by gamma-secretase. J. Biol. Chem. **283:**29627–29631.
40. **Struhl, G., and A. Adachi.** 2000. Requirements for presenilin-dependent cleavage of notch and other transmembrane proteins. Mol. Cell **6:**625–636.
41. **Takasugi, N., T. Tomita, I. Hayashi, M. Tsuruoka, M. Niimura, Y. Takahashi, G. Thinakaran, and T. Iwatsubo.** 2003. The role of presenilin cofactors in the gamma-secretase complex. Nature **422:**438–441.
42. **Thinakaran, G., and E. H. Koo.** 2008. Amyloid precursor protein trafficking, processing, and function. J. Biol. Chem. **283:**29615–29619.
43. **Wakabayashi, T., K. Craessaerts, L. Bammens, M. Bentahir, F. Borgions, P. Herdewijn, A. Staes, E. Timmerman, J. Vandekerckhove, E. Rubinstein, C. Boucheix, K. Gevaert, and B. De Strooper.** 2009. Analysis of the gamma-secretase interactome and validation of its association with tetraspanin-enriched microdomains. Nat. Cell Biol. **11:**1340–1346.
44. **Winkler, E., S. Hobson, A. Fukumori, B. Dumpelfeld, T. Luebbers, K. Baumann, C. Haass, C. Hopf, and H. Steiner.** 2009. Purification, pharmacological modulation, and biochemical characterization of interactors of endogenous human gamma-secretase. Biochemistry **48:**1183–1197.
45. **Wolfe, M. S.** 2009. Gamma-secretase in biology and medicine. Semin. Cell Dev. Biol. **20:**219–224.
46. **Wolfe, M. S., W. Xia, B. L. Ostaszewski, T. S. Diehl, W. T. Kimberly, and D. J. Selkoe.** 1999. Two transmembrane aspartates in presenilin-1 required for presenilin endoproteolysis and gamma-secretase activity. Nature **398:** 513–517.
47. **Wrigley, J. D., I. Schurov, E. J. Nunn, A. C. Martin, E. E. Clarke, S. Ellis, T. P. Bonnert, M. S. Shearman, and D. Beher.** 2005. Functional overexpression of gamma-secretase reveals protease-independent trafficking functions and a critical role of lipids for protease activity. J. Biol. Chem. **280:**12523–12535.
48. **Xia, W., W. J. Ray, B. L. Ostaszewski, T. Rahmati, W. T. Kimberly, M. S. Wolfe, J. Zhang, A. M. Goate, and D. J. Selkoe.** 2000. Presenilin complexes with the C-terminal fragments of amyloid precursor protein at the sites of amyloid beta-protein generation. Proc. Natl. Acad. Sci. U. S. A. **97:**9299–9304.
49. **Yu, G., F. Chen, G. Levesque, M. Nishimura, D. M. Zhang, L. Levesque, E. Rogaeva, D. Xu, Y. Liang, M. Duthie, P. H. St George-Hyslop, and P. E. Fraser.** 1998. The presenilin 1 protein is a component of a high molecular weight intracellular complex that contains beta-catenin. J. Biol. Chem. **273:** 16470–16475.